 doi:10.20944/preprints202205.0231.v1

Article

Yield predictions of four hybrids of maize (*Zea mays*) using multispectral images obtained from RPAS in the coast of Peru

David Saravia [1,2], Wilian Salazar [1], Lamberto Valqui-Valqui [1], Javier Quille-Mamani [1,3], Rossana Porras-Jorge [1,2], Flor-Anita Corredor [1], Elgar Barboza [1,4], Héctor V. Vásquez [1] and Carlos I. Arbizu [1,*]

[1] Dirección de Desarrollo Tecnológico Agrario, Instituto Nacional de Innovación Agraria (INIA), Av. La Molina, 1981, Lima 15024, Peru; wilian-salazar@hotmail.es (W.S.); lambertovalqui@gmail.com (L.V-V.); corredor@alumni.iastate.edu (F-A.C.); hvasquez@inia.gob.pe (H.V.V.)
[2] Facultad de Agronomía, Universidad Nacional Agraria La Molina, Av. La Molina s/n, Lima 15024, Lima, Perú; dsaravia@lamolina.edu.pe (D.S.); zrporras@lamolina.edu.pe (R.P-J.)
[3] Grupo de Cartografía GeoAmbiental y Teledetección, Universitat Politècnica de València, Camí de Vera s/n, 46022, Valencia, España; jaquille@upv.es (J.Q-M.)
[4] Instituto de Investigación para el Desarrollo Sustentable de Ceja de Selva (INDES-CES), Universidad Nacional Toribio Rodríguez de Mendoza de Amazonas (UNTRM), Chachapoyas 01001, Peru; ebarboza@indes-ces.edu.pe (E.B.)
* Correspondence: carbizu@inia.gob.pe; Tel.: +51 979 371 014

Abstract: Early assessment of crop development is a key aspect of precision agriculture. Shortening the time of response before a deficit of irrigation, nutrients and damage by diseases is one of the usual concerns in agriculture. Early prediction of crop yields can increase profitability in the farmer's economy. In this study we aimed to predict the yield of four maize commercial hybrids (Dekalb7508, Advanta9313, MH_INIA619 and Exp_05PMLM) using remotely sensed spectral vegetation indices (VI). A total of 10 VI (NDVI, GNDVI, GCI, RVI, NDRE, CIRE, CVI, MCARI, SAVI, and CCCI) were considered for evaluating crop yield and plant cover at 31, 39, 42, 46 and 51 days after sowing (DAS). A multivariate analysis was applied using principal component analysis (PCA), linear regression, and r-Pearson correlation. In the present study, highly significant correlations were found between plant cover with VIs at 46 (GNDVI, GCI, RVI, NDRE, CIRE and CCCI) and 51 DAS (GNDVI, GCI, NDRE, CIRE, CVI, MCARI and CCCI). The PCA indicated a clear discrimination of the dates evaluated with VIs at 31, 39 and 51 DAS. The inclusion of the CIRE and NDRE in the prediction model contributed to estimate the performance, showing greater precision at 51 DAS. The use of RPAS to monitor crops allows optimizing resources and helps in making timely decisions in agriculture in Peru.

Keywords: vegetation indices; precision farming; hybrid; phenotyping; remote sensing

1. Introduction

World population growth is constant over time, with estimates of 9.7 billion people by 2050 and 11 billion by 2100 [1]. Therefore, it is essential to strengthen food security, increasing crop production through the efficient use of resources for its sustainability. In this sense, corn is one of the most important cereals in the world and a staple food in many households. It is also a source in animal feed and a fundamental product in the food industry [2,3]. World production is estimated at 1,192 Mt, with the largest producers being the United States, China, Brazil and Mexico [4].

In the last decade, the use of technologies in agriculture has also increased significantly through the usage of geographic information systems (GIS), and global navigation satellite systems (GNSS), remote sensing, RPAS, machinery and other technologies that have supported precision agriculture [5–7]. The incorporation of these disciplines allows the collection, processing and analysis of temporal, spatial and individual data and combines them with other data for the implementation of adequate solutions in the use of

 doi:10.20944/preprints202205.0231.v1

resources, productivity, quality, profitability and sustainability of agricultural production [8–11].

A wide range of RPAS and satellite-mounted sensors have been used in phenotyping studies to obtain aerial images and monitor crop development [12,13]. Landsat and Sentinel-2 satellites collect images in the red wavelength and near infrared (NIR) to assess the health of crop development on a regional and global scale [14–17]. However, the spatial resolution has not been fine enough to meet the phenotypic measurement needs of various research projects in crops and in small areas at the level of small agricultural producers [12,18]. For this reason, the use of RPAS is currently gaining prestige as an integral part of precision agriculture, guaranteeing successful harvests [19].

On the other hand, RPAS with remote sensors can collect detailed information on the phenological development of crops through high spatial and temporal resolution images, which greatly reduces labor and time costs [20–22]. These sensors can acquire bands such as thermal infrared, RGB band, NIR band and red edge (RE) band [19]. These bands allow studying biomass growth, nitrogen content, yield, water stress and chlorophyll measurement in citrus, corn, wheat, soybean and grapevine crops [11,22–27], through the application of vegetation indices (VI) such as the normalized difference vegetation index (NDVI) and others based on reflectance [12].

Precise estimation of maize yield at a local or regional scale helps improve food security and develop more supportive models [28]. In Peru, the cultivated area of corn during the 2019 - 2020 season was 237,000 hectares with a production of 1.1 Mt per hectare (SIEA, 2021). Recently, maize cultivation has become highly susceptible to climate change conditions with strong variations in yield over the years [29]. It is also subject to the limited availability of technologies that help in the detection, monitoring and analysis of the crop. In this context, the use of RPAS and multispectral sensors are an excellent option to evaluate and estimate the production of this crop [30]. Consequently, in this study we evaluate the performance of four maize hybrids in the Peruvian coast, by applying VI calculated from multispectral images obtained from RPAS.

2. Materials and Methods

2.1. Study area

The data collection was carried out at the Centro Experimental La Molina (CELM) of the Instituto Nacional de Innovación Agraria (INIA) (-12° 4' W, -76° 56' S) (Figure 1), which is located in the district of La Molina, province and department of Lima (Peru).

This area is characterized by a semi-arid climate, presenting an annual rainfall of 5.7 mm and an average temperature of 17.3 °C in 2021 (CELM Automatic Weather Station). The type of soil is sandy loam with physical characteristics of electrical conductivity (EC) of 1.59 dS/m, pH 7.32, field capacity 14.8%, wilting point 7.7% and apparent density of 1.54 g/cm^3 (INIA Water, Soil and Foliar Research Laboratory).

Preprints (www.preprints.org) | NOT PEER-REVIEWED | Posted: 17 May 2022 doi:10.20944/preprints202205.0231.v1

Figure 1. Location of the study area the La Molina Experimental Center in Lima (Peru).

The experimental field consisted of 48 research units installed with four maize commercial hybrids (Dekalb7508, Advanta9313, MH_INIA619 and Exp_05PMLM). They have a vegetative period of approximately 120 days and adapt very well to different regions of the Peruvian coast. Each unit represented an area of 32.8 m² (8 m long and 4.1 m wide) with five furrows spaced 0.9 m apart and between plant bumps at 0.25 m. The season of greater planting of the crop is carried out in spring-summer. The evaluation and monitoring of the field experiment began with sowing on January 18, 2021, to end with its harvest on May 31 of the same year. During the vegetative period, the maximum temperature recorded was 30.4 °C in January, while the minimum was 15 °C in June.

A drip irrigation system was used, with a drip flow rate of 3.7 l/h and a distance between drippers of 0.2 m. Management practices such as weed and pest control were carried out manually and the use of herbicides as part of the agronomic management of the field.

2.2. Data collection

Yield data was obtained from a representative area of 32.8 m² in each experimental unit, which was then expressed as t/ha. The process consisted of weighting the total corn grains of each plot, and then extracting a 200 g sample to be dried in an oven at 60°C for an interval of 72 hours, reaching a grain moisture of approximately 10% to estimate yield per hectare.

Images obtained from the RPAS covered the different stages of maize development, which were taken at a height of 30 meters. They were collected between 11:00 a.m. and 2:00 p.m. to minimize changes in the solar zenith angle in cloudless weather conditions [31]. Five dates were selected for the acquisition of the images at 31, 39, 42, 46 and 51 DAS between the months of January to March 2021. The RPAS Phanthon 4 Pro (https://www.dji.com/phantom-4-pro?site=brandsite&from=nav, Shenzhen, China, accessed on 22 March 2022) coupled with Parrot Sequoia multispectral camera (Parrot SA, París, France) was used to acquire the images of the 48 study units.

Preprints (www.preprints.org) | NOT PEER-REVIEWED | Posted: 17 May 2022 doi:10.20944/preprints202205.0231.v1

Four bands were acquired in the wave ranges from 530 to 570 nm (Green); 640 to 680 nm (Red); 730 to 740 nm (Red edge); 770 to 810 nm (Near-Infrared), all at a multispectral image´ spatial resolution of 1 megapixels [32].

For the acquisition of precise images, a luminosity sensor located in the upper part of the RPAS was used. The flight plan was designed with a 75% overlap between images. On the other hand, for the georeferencing of the images, seven ground control points (GCPs) were used, which were measured using a high-precision GNSS, which were marked with topographic targets [33].

Figure 2. Equipment used in data collection. RPAS and radio control, and Parrot Sequoia camera.

2.3. Canopy cover estimation

To calculate the canopy cover, the Image Classification, Editor, and spatial analysis tools (Spatial Analyst Tools) of the ArcMap software (ArcGiS 10.4.1) were used. Manual classification of the images (Achicanoy et al., 2018) was carried out in three classes (vegetation cover, soil and shade). From these, an output surface map with the vegetation cover was generated, which allowed calculating the corn cover percentages from the mosaic of photos obtained with the Phantom 4 drone for each date of images generated in the field.

2.4. Vegetation indices estimation

The multispectral images of the RPAS missions were made with the software Pix4D Capture (flight plan management) and processed in the Pix4Dmapper (V4.5.6, Pix4D S.A., Prilly, Switzerland) that allowed to generate the orthomosaic. We also performed the geometric correction and obtained the reflectance values [25]. Before calculating the VI, the supervised classification was applied identifying i) maize, ii) weeds, iii) shade, and iv) soil, which allowed determining the maize cover [34]. The VI were estimated within the area of the corn cover that was previously extracted through spatial mask extraction processing in the software ArcGIS 10.5. In the Table 1 shows the indices evaluated on the five study dates.

Table 1. Vegetación indices applied for corn yield evaluation.

Índices	Ecuación	Fuente
Normalized Difference Vegetation Index (NDVI)	$NDVI = \frac{NIR - Red}{NIR + Red}$	[35]
Green Normalized Difference Vegetation Index (GNDVI)	$GNDVI = \frac{NIR - Green}{NIR + Green}$	[36]
Green Chlorophyll Index (GCI)	$GCI = \frac{NIR}{Green} - 1$	[37]

Preprints (www.preprints.org) | NOT PEER-REVIEWED | Posted: 17 May 2022 doi:10.20944/preprints202205.0231.v1

Ratio Vegetation Index (RVI)	$RVI = \frac{NIR}{Red}$	[38]
Normalized Difference RedEdge Index (NDRE)	$NDRE = \frac{NIR - Rededge}{NIR + Rededge}$	[39]
ChlorophyII Index-RedEdge (CIRE)	$CIRE = \frac{NIR}{Rededge} - 1$	[37]
ChlorophyII Vegetation Index (CVI)	$CVI = \frac{NIR * Red}{Green^2}$	[40]
Modified Chlorophyll Absorption Reflectance Index (MCARI)	$MCARI = [(Rededge - red) - 0.2 * (Rededge - green) * \frac{Rededge}{Red}$	[41]
Soil Adjusted Vegetation Index (SAVI)	$SAVI = \frac{(NIR - Red)(1 + L)}{NIR + Red + L}$	[42]
Canopy Chlorophyll Content Index (CCCI)	$CCCI = \frac{\frac{NIR - Rededge}{NIR + Rededge}}{\frac{NIR - Red}{NIR + Red}}$	[43]

2.5. Data analysis and model development

Firstly, agronomical yield measurement for each corn hybrid were estimated based on the weights of dry grain of corn expressed in tons per hectare. The averages and standard error for each hybrid and the comparison of means was carried out by a Duncan.test with alpha=0.05.

The canopy cover and VIs were estimated from the multispectral at 31, 39, 42, 46 and 51 DAS. A Duncan.test means comparison was performed among corn hybrids on each date evaluated. With the data over time, box plot graphs were constructed over the five dates for each variable evaluated in the experiment.

A principal component analysis (PCA) was performed to determine the variations between each VI over time and determine the most relevant index in predicting yield. Subsequently, the r-Pearson correlation was applied to the indices with greater performance accuracy. Finally, the yield means between the four maize varieties were compared using Duncan's test with con α=0.05. We used the following libraries within R, [44] *factoMineR* [45], *ggplot2* [46], *factoextra* [47], *GGally* [48], *Hmisc* [49] and *agricolae* [50].

3. Results

3.1. Yield for each corn hybrid and canopy cover estimation

Figure 3 shows the results of applying the Duncan test to compare the means of yield per hybrid at 51 DAS and the percentage of canopy cover, according to DAS and VI. Two groups without significant differences were identified, the first consisting of Advanta9313 (9.91 ± 2.15 t/ha) and Dekalb7508 (8.85 ± 1.38 t/ha), and the second MH_INIA619 (6.23 ± 1.51 t/ha) and Exp_05MLM (5.81 ± 1.21 t/ha) (Figure 3a). The yield varies from 5.81 to 9.91 t/ha. The hybrids Advanta9313 and Decalb7508 presented the highest performance and hybrid Exp_05MLM reported the lowest (Figure 3b). At the level of canopy coverage at 31 DAS, the hybrid Exp_05MLM presented greater coverage, followed by Dekalb7508 and MH_INIA619. Dekalb7508 presented greater canopy coverage at 39 and 46 DAS. However, at 51 DAS the canopy cover for the four hybrids were similar.

Preprints (www.preprints.org) | NOT PEER-REVIEWED | Posted: 17 May 2022 doi:10.20944/preprints202205.0231.v1

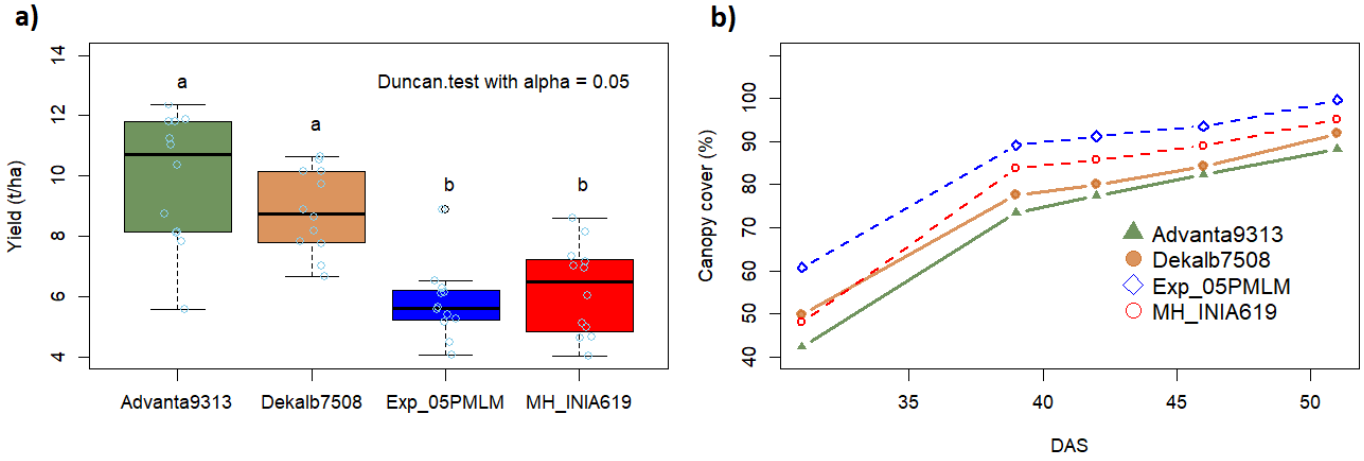

Figure 3. Comparison of crop yield and canopy cover according to maize hybrid. a) Crop yield of the four corn hybrids with Duncan.test $\alpha = 0.05$; b) plot of Canopy cover according to hybrid, at 31, 39, 42, 46 and 51 DAS.

3.2. Vegetation indices estimations and canopy cover relationships

The canopy cover according to the DAS is shown in Figure 4a. Greater variability of canopy cover at 31 DAS is presented, which improved at 51 DAS. The correlation between the VI with the DAS (Figures 4b-k) indicated that the reflectance values for nine indices increased cumulatively with the advance of the vegetative period. Only the MCARI reported a decrease at 42 DAS. The GNDVI, GCI, RVI, NDRE, CIRE and CCCI indices) showed high significance of plant cover at 46 DAS and the GNDVI, GCI, NDRE, CIRE, CVI, MCARI and CCCI indices at 51 DAS.

Preprints (www.preprints.org) | NOT PEER-REVIEWED | Posted: 17 May 2022 doi:10.20944/preprints202205.0231.v1

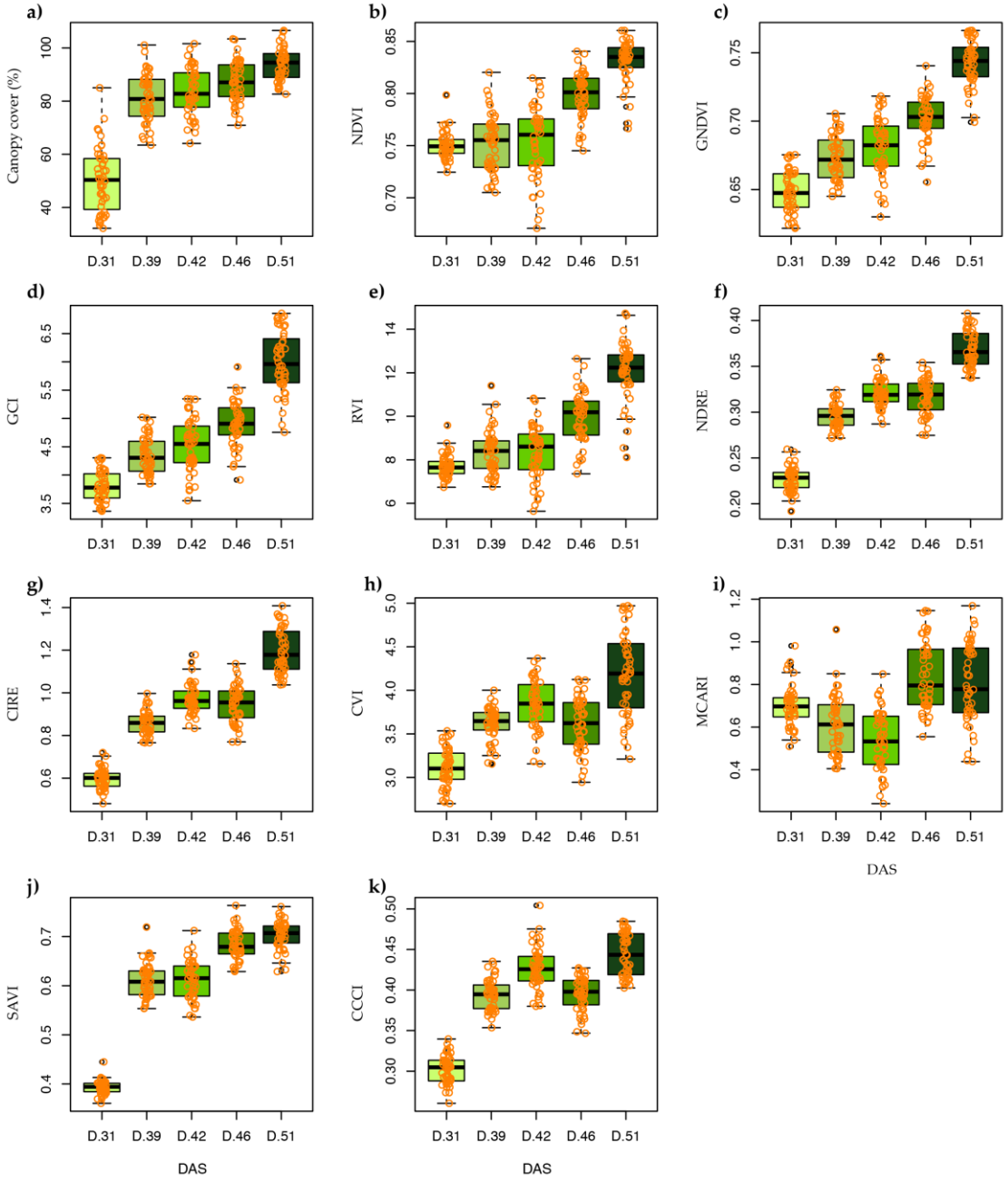

Figure 4. Comparison of canopy cover according to DAS and vegetation indices; a) Canopy cover; b) NDVI; c) GNDVI, d) GCI; e) RVI, f) NDRE; g) CIRE, h) CVI; i) MCARI; j) SAVI; k) CCCI.

3.3. Development of prediction models to calculate crop yields

Table 2 shows the r-Pearson correlation between DAS, canopy cover and VI. The highest correlation between DAS and canopy cover occurs at 39 and 51 DAS with -0.41 and -0.43, respectively. The SAVI (-0.32) and MACARI (-0.36) indices presented a minor correlation at 31 and 51 DAS. On the other hand, the GNDVI (0.42) and GCI (0.41) indices presented correlations of medium importance. The NDRE (0.58), CIRE (0.57) and CCCI (0.54) indices reported a highly significant correlation at 46 DAS. Likewise, at 51 DAS, the GNDVI (0.55), GCI (0.57), NDRE (0.78), CIRE (0.78), CVI (0.52) and CCCI (0.64) indices showed a very significant correlation.

Preprints (www.preprints.org) | NOT PEER-REVIEWED | Posted: 17 May 2022 doi:10.20944/preprints202205.0231.v1

Table 2. r-Pearson correlation between corn yield with canopy cover and vegetation indices.

DAS	C_cover	NDVI	GNDVI	GCI	RVI	NDRE	CIRE	CVI	MCARI	SAVI	CCCI
31	-0.28	-0.22	-0.05	-0.03	-0.18	0.26	0.24	0.11	-0.44**	-0.32*	0.33
39	-0.41**	-0.10	0.03	0.07	-0.01	0.21	0.19	0.19	-0.20	-0.20	0.27
42	-0.30*	0.11	0.14	0.16	0.16	0.23	0.24	0.04	-0.05	-0.02	0.08
46	-0.28	0.29	0.42**	0.41**	0.31*	0.58***	0.57***	0.28	-0.16	0.03	0.54***
51	-0.43**	0.15	0.55***	0.57***	0.25	0.78***	0.78***	0.52***	-0.36*	-0.10	0.64***

* *P* value < 0.05 ** *P* value < 0.01 *** *P* value < 0.001.

The relationship between crop yield and VI is shown in Table 3. The NDVI, MCARI and SAVI indices reported highly significant correlations for all evaluation days. In turn, correlation for the GNDVI, GCI, RVI indices at 51 DAS varies from very significant to medium importance. However, for the CVI and CCCI indices, the correlation increases according to the DAS.

Table 3. r-Pearson correlation between corn yield with vegetation indices.

DAS	NDVI	GNDVI	GCI	RVI	NDRE	CIRE	CVI	MCARI	SAVI	CCCI
31	0.81***	0.51***	0.50***	0.78***	0.45**	0.46***	0.09	0.77***	0.88***	0.24
39	0.84***	0.66***	0.61***	0.75***	0.15	0.19	0.19	0.84***	0.88***	-0.53***
42	0.71***	0.61***	0.58***	0.72***	0.11	0.17	-0.22	0.82***	0.86***	-0.55***
46	0.69***	0.38*	0.34*	0.62***	0.05	0.08	-0.36*	0.80***	0.80***	-0.32*
51	0.55***	0.05	-0.02	0.42**	-0.45**	-0.42**	-0.48***	0.73***	0.73***	-0.64***

* *P* value < 0.05 ** *P* value < 0.01 *** *P* value < 0.001.

The results of the PCA are presented in Figure 5 for the five dates evaluated. There is a variability of the VI according to the temporality, the greater the distance from the calculation, the greater the difference between them. For comparison, on days 31, 39 and 51 DAS, there is no group overlap (Figure 5a), indicating a clear discrimination of the groups in this multivariate analysis. However, the opposite occurs at 39, 42 and 46 DAS, where there is an overlap because they are very close dates that do not allow a clear discrimination of the indices generated on the maize plant cover.

When performing the PCA for the canopy cover and yield indices at each date of the generated images (Figures 5b-e), we observe that there is no clear discrimination of groups with respect to the maize hybrids evaluated, but at 51 DAS (Figure 5f) two groups are observed. The corn yield at 51 DAS goes in the same direction as most VI, which is also reflected in the correlations with greater significance for that date (Table 2).

Preprints (www.preprints.org) | NOT PEER-REVIEWED | Posted: 17 May 2022 doi:10.20944/preprints202205.0231.v1

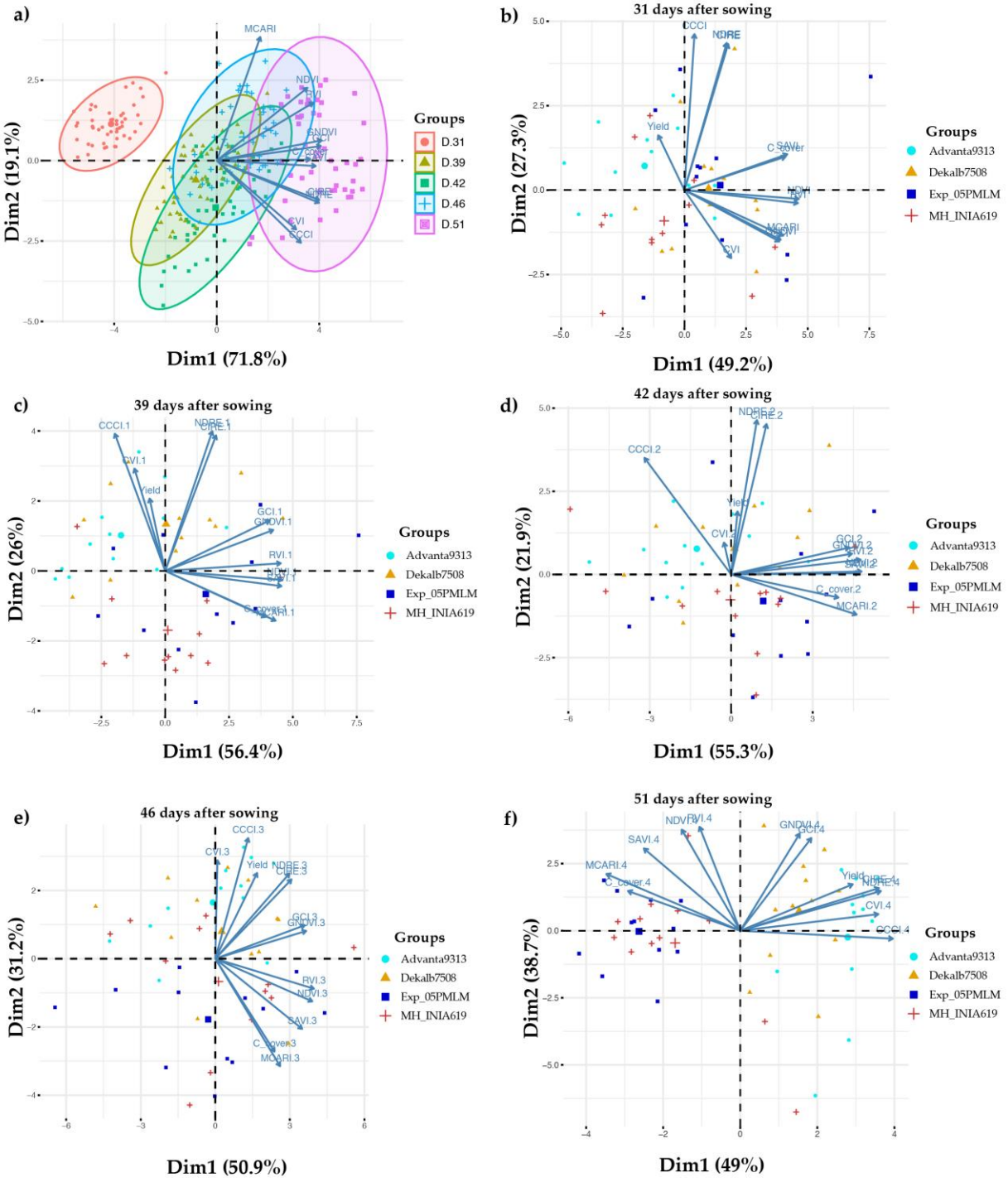

Figure 5. PCA for VI during the evaluation days, a) PCA for the indices and DAS, b) PCA for the indices and group of hybrids at 31 DAS; c) PCA for the indices and group of hybrids at 39 DAS; c) PCA for the indices and group of hybrids at 42 DAS; d) PCA for the indices and group of hybrids at 46 DAS; e) PCA for the indices and group of hybrids at 51 DAS.

Based on the indices that presented significant correlations with a P value > 0.45 (GCI, NDRE, CIRE and CCCI), two crop yield prediction models were built at 46 and 51 DAS. Model 1 was built based on the NDRE, CIRE and CCCI indices at 46 DAS, which reported a coefficient of determination (R^2) of 0.34 (Figure 6a) and does not show a significant increase per index (Figures 6b-d). In turn, model 2 was built from the GCI, NDRE and CIRE indices at 51 DAS with an R^2 of 0.62 (Figure 6e). However, at the index level, the GCI

Preprints (www.preprints.org) | NOT PEER-REVIEWED | Posted: 17 May 2022 doi:10.20944/preprints202205.0231.v1

reports the lowest R2 (R^2 = 0.33) (Figure 6f) with respect to the NDRE and CIRE, which presented R^2 values of 0.61 (Figures 6g-h).

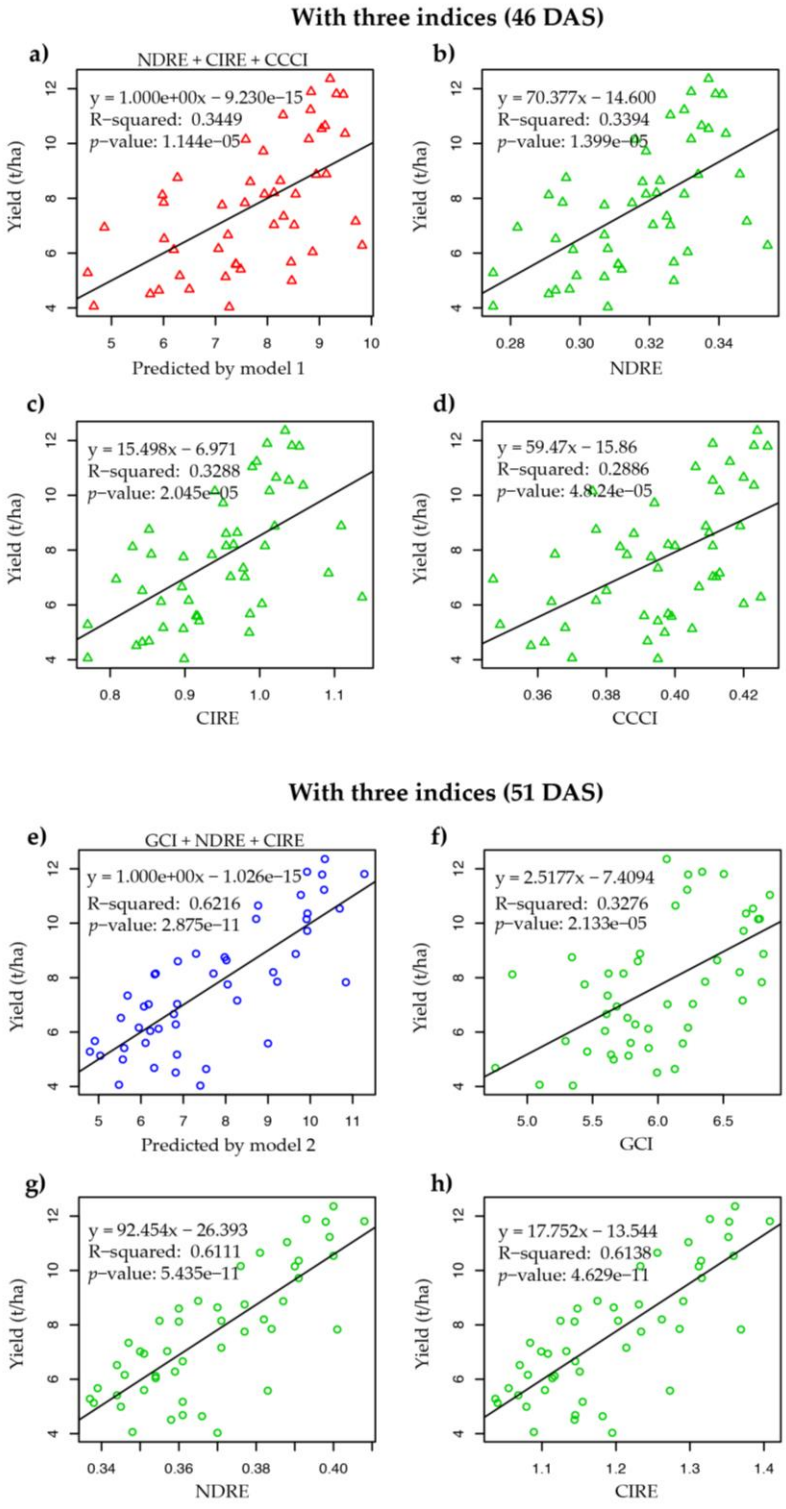

Figure 6. Maize yield prediction models with multiple linear regression; a) Model 1 for performance prediction using the NDRE, CIRE and CCCI indices at 46 DAS; b) Model 1 for performance prediction using NDRE at 46 DAS; c) Model 1 for performance prediction using CIRE at 46 DAS; d) Model 1 for performance prediction using CCCI at 46 DAS; e) Model 2 for performance prediction using the GCI, NDRE and CIRE indices at 51 DAS; f) Model 2 for performance prediction using GCI at 51 DAS; g) Model 2 for performance prediction using NDRE at 51 DAS; h) Model 2 for performance prediction using CIRE at 51 DAS.

 doi:10.20944/preprints202205.0231.v1

4. Discussion

The use of multispectral images obtained from RPAS allowed the prediction of the yield of the maize crop in this study. One of the advantages of using RPAS in the monitoring of experimental plots or crops is that it can be controlled remotely and generates lower maintenance costs and acquisition of high-resolution images [51]. Hybrid Advanta9313 (9.91 t/ha) presented the highest yield at 51 DAS, a value higher than the national average of 4.77 t/ha [52] and similar to those reported by Gavilánez-Luna & Gómez-Vargas[53]. This superiority in yield performance could be due to its wide adaptability to the maize areas of Peru and its good production stability [54].

For the estimation of canopy cover in the experimental plot, a total of 10 VIs were selected (Table 1). VIs were calculated using multispectral reflectance measurements at visible and near-infrared wavelengths. This range of lengths have been used in different precision agriculture applications such as plant counting, growth monitoring, phenology and chlorophyll measurement. [24,31,51,55,56]. At the VI level, it is observed that at 46 and 51 DAS, there are high significant correlations, since, at this stage, the chlorophyll content also increases significantly, as does the canopy cover. In nine indices, values increased cumulatively with advancing growing season. Only the MCARI showed a decrease at 42 DAS. The NDVI values ranged from 0.75 to 0.83 throughout the evaluation, unlike the GNDVI that went from 0.65 to 0.75, the SAVI being very similar to the NDVI on the first date evaluated. The average values were 0.4 and for the 51 DAS they oscillated around 0.70.

In regards to calculated linear regression models, better results were obtained at 51 DAS and only when they were generated from a single vegetation index. Indices NDRE and CIRE presented the highest R^2 (0.61) with the following models: 92.454*NDRE-26.393 and 17.752*CIRE-13.544. On the other hand, the R^2 values are lower than those obtained by Barzin et al. [57], who used the index OSAVI y SCCCI. At the same time Sunoj et al. [58] used exponential and nonlinear NDVI models for yield prediction and obtained R^2 values greater than 0.90. The lower correlations in the early stage may be due to the fact that the physiological characteristics of maize do not yet show significant differences. In other studies, they used satellite images such as MODIS and Landsat 8, where they found high performance predictions at 65-75 and 60-62 DAS, respectively [26,59].

The NDVI showed a low correlation (0.15) for yield estimation. However, higher NDVI values (0.53) have been reported in other studies, this may be due to the location and range of the electromagnetic spectrum taken by the Parrot Sequoia camera [27]. These results are also different from those obtained in wheat crops where the NDVI values fluctuated from 0.40, 0.49 and 0.45, for the early, intermediate and late grain-filling stages for full irrigation treatment [60]. In another study carried out with Landsat images, the indices that best predicted corn crop yield were Enhanced Vegetation Index (EVI), SAVI and Optimized Soil-Adjusted Vegetation Index (OSAVI), which were different from the NDVI [61]. Through the use of Landsat-7 ETM+ and Spot 5 images, they found high correlation values of the NDVI index in the yield of sugarcane, sugar and barley [62,63].

At small spatial scales, our study provided insight into the potential of using remotely sensed spectral VI from RPAS' multispectral images for monitoring and estimating maize field yield. RPAS and multispectral cameras can provide substantial spatial data on crop yield and quality at low cost [64]. In addition, they provided an opportunity to monitor farmers' plots, where crop monitoring is limited. Finally, this study opens new doors for the development of research and practical applications of drones in agriculture for all the three regions of Peru: costa, sierra and selva (coast, highlands and Amazon).

5. Conclusions

Results indicated a highly significant correlation between canopy cover and 10 VIs derived from RPAS multispectral images. Performance showed high correlations at 46 DAS with six indices (GNDVI, GCI, RVI, NDRE, CIRE and CCCI) and at 51 DAS with seven indices (GNDVI, GCI, NDRE, CIRE, CVI, MCARI and CCCI). Prediction models for performance from multiple correlations at 46 and 51 DAS were similar when three indices or just one were used. The PCA indicated a clear discrimination of the dates evaluated with the VI at 31, 39 and 51 DAS. The corn hybrids Dekalb7508 and Advanta9313 presented better performance than MH_INIA619 and Exp_05PMLM. Corn yield showed a high correlation during the reproductive stage (46 and 51 DAS) with the indices (GNDVI, GCI, RVI, NDRE, CIRE, CVI, MCARI and CCCI). In short, when compared to manual evaluation, VIs will allow timely decisions to be made when monitoring corn crops.

Author Contributions: Conceptualization, R.P.-J.; Data curation, D.S., J.Q.-M. and C.I.A.; Formal analysis, D.S. and L.V.-V.; Investigation, W.S., J.Q.-M., R.P.-J., F.-A.C., E.B. and C.I.A.; Methodology, D.S., W.S., L.V.-V., J.Q.-M., R.P.-J. and E.B.; Project administration, H.V. and C.I.A.; Resources, H.V.; Supervision, W.S., R.P.-J., F.-A.C., E.B. and H.V.; Validation, C.I.A.; Writing – original draft, D.S., L.V.-V., J.Q.-M., R.P.-J., F.-A.C., E.B. and C.I.A.; Writing – review & editing, D.S., W.S., L.V.-V., J.Q.-M., R.P.-J., F.-A.C., E.B. and H.V..

Funding: This research was funded by the project "Creación del servicio de agricultura de precisión en los Departamentos de Lambayeque, Huancavelica, Ucayali y San Martín 4 Departamentos" of the Ministry of Agrarian Development and Irrigation (MIDAGRI) of the Peruvian Government with grant number CUI 2449640.

Data Availability Statement: All data generated during this study are included in this published article.

Acknowledgments: We thank Ivan Ucharima for image processing, and "Centro Experimental La Molina" for providing field resources. In addition, we thank Eric Rodriguez, Maria Angélica Puyo and Cristina Aybar for supporting the logistic activities in our laboratory.

Conflicts of Interest: The authors declare no conflict of interest.

References

1. Naciones Unidas. Paz, dignidad e igualdad en un planeta sano. Una población en crecimiento. Available online: https://www.un.org/es/sections/issues-depth/population/index.html (accessed on 18 April 2022).
2. Obour, P.B.; Arthur, I.K.; Owusu, K. The 2020 Maize Production Failure in Ghana: A Case Study of Ejura-Sekyedumase Municipality. *Sustainability.* **2022**, *14*, 3514, doi:10.3390/su14063514.
3. Zhao, M.; Bingcan, C. Corn Oil. *Ref. Modul. Food Sci.* **2022**, *22*, doi: 10.1016/B978-0-12-823960-5.00013-5.
4. FAO. Nota informativa de la FAO sobre la oferta y la demanda de cereales. Available online: https://www.fao.org/worldfoodsituation/csdb/es/ (accessed on 10 April 2022).
5. Ahmad, A.; Ordoñez, J.; Cartujo, P.; Martos, V. Remotely piloted aircraft (RPA) in agriculture: A pursuit of sustainability. *Agronomy.* **2020**, *11*, doi:10.3390/agronomy11010007.
6. Carrer, M.J.; Filho, H.M. de S.; Vinholis, M. de M.B.; Mozambani, C.I. Precision agriculture adoption and technical efficiency: An analysis of sugarcane farms in Brazil. *Technol. Forecast. Soc. Change.* **2022**, *177*, doi:10.1016/j.techfore.2022.121510.
7. Manlove, J.L.; Shew, A.M.; Obembe, O.S. Arkansas producers value upload speed more than download speed for precision agriculture applications. *Comput. Electron. Agric.* **2021**, *190*, 106432, doi:10.1016/j.compag.2021.106432.
8. Erickson, B.; Fausti, S.W. The role of precision agriculture in food security. *Agron. J.* **2021**, *113*, 4455–4462, doi:10.1002/agj2.20919.
9. Urbahs, A.; Jonaite, I. Features of the use of unmanned aerial vehicles for agriculture applications. *Aviation* . **2013**, *17*, 170–175, doi:10.3846/16487788.2013.861224.
10. Tey, Y.S.; Brindal, M. Factors influencing the adoption of precision agricultural technologies: a review for policy implications. *Precis. Agric.* **2012**, *13*, 713–730, doi:10.1007/s11119-012-9273-6.
11. Haghverdi, A.; Washington-Allen, R.A.; Leib, B.G. Prediction of cotton lint yield from phenology of crop indices using artificial neural networks. *Comput. Electron. Agric.* **2018**, *152*, 186–197, doi:10.1016/j.compag.2018.07.021.
12. Wu, G.; Miller, N.D.; de Leon, N.; Kaeppler, S.M.; Spalding, E.P. Predicting *Zea Mays* flowering time, yield, and kernel dimensions by analyzing aerial images. *Front. Plant Sci.* **2019**, *10*, 1–12, doi:10.3389/fpls.2019.01251.
13. Danilevicz, M.F.; Bayer, P.E.; Boussaid, F.; Bennamoun, M.; Edwards, D. Maize yield prediction at an early developmental stage using multispectral images and genotype data for preliminary hybrid selection. *Remote Sens.* **2021**, *13*, doi:10.3390/rs13193976.

14. Wulder, M.A.; Masek, J.G.; Cohen, W.B.; Loveland, T.R.; Woodcock, C.E. Opening the archive: How free data has enabled the science and monitoring promise of Landsat. *Remote Sens. Environ.* **2012**, *122*, 2–10, doi:10.1016/j.rse.2012.01.010.
15. Guo, W.; Maas, S.J.; Bronson, K.F. Relationship between cotton yield and soil electrical conductivity, topography, and Landsat imagery. *Precis. Agric.* **2012**, *13*, 678–692, doi:10.1007/s11119-012-9277-2.
16. Soriano-González, J.; Angelats, E.; Martínez-Eixarch, M.; Alcaraz, C. Monitoring rice crop and yield estimation with Sentinel-2 data. *F. Crop. Res.* **2022**, *281*, 108507, doi:10.1016/j.fcr.2022.108507.
17. Marshall, M.; Belgiu, M.; Boschetti, M.; Pepe, M.; Stein, A.; Nelson, A. Field-level crop yield estimation with PRISMA and Sentinel-2. *ISPRS J. Photogramm. Remote Sens.* **2022**, *187*, 191–210, doi:10.1016/j.isprsjprs.2022.03.008.
18. Han-Ya, I.; Ishii, K.; Noguchi, N. Satellite and aerial remote sensing for production estimates and crop assessment. *Environ. Control Biol.* **2010**, *48*, 51–58, doi:10.2525/ecb.48.51.
19. Rani, A.; Chaudhary, A.; Sinha, N.K.; Mohanty, M.; Chaudhary, R.S. Drone : The green technology for future agriculture. *Soil Helath Technol. Interv.* **2019**, *2*, 3–6.
20. Du, M.; Noguchi, N. Monitoring of wheat growth status and mapping of wheat yield's within-field spatial variations using color images acquired from UAV-camera system. *Remote Sens.* **2017**, *9*, doi:10.3390/rs9030289.
21. Deery, D.; Jimenez-Berni, J.; Jones, H.; Sirault, X.; Furbank, R. *Proximal Remote Sensing Buggies and Potential Applications for Field-Based Phenotyping*; 2014; Vol. 4; ISBN 6126246497.
22. Montes, J.M.; Technow, F.; Dhillon, B.S.; Mauch, F.; High-throughput non-destructive biomass determination during early plant development in maize under field conditions. *F. Crop. Res.* **2011**, *121*, 268–273, doi:10.1016/j.fcr.2010.12.017.
23. Pölönen, I.; Saari, H.; Kaivosoja, J.; Honkavaara, E.; Pesonen, L. Hyperspectral imaging based biomass and nitrogen content estimations from light-weight UAV. *Remote Sens. Agric. Ecosyst. Hydrol. XV.* **2013**, *8887*, 88870J, doi:10.1117/12.2028624.
24. Pino, E.V. Los drones una herramienta para una agricultura eficiente: un futuro de alta tecnología. *Idesia (Arica).* **2019**, 37, 75-85, doi:10.4067/s0718-34292019005000402.
25. Zaigham, S.M.; Awais, M.; Khan, F.S.; Afzal, U.; Naz, N.; Khan, M.I. Unmanned air vehicle based high resolution imagery for chlorophyll estimation using spectrally modified vegetation indices in vertical hierarchy of citrus grove. *Remote Sens. Appl. Soc. Environ.* **2021**, *23*, 100596, doi:10.1016/j.rsase.2021.100596.
26. Bolton, D.K.; Friedl, M.A. Forecasting crop yield using remotely sensed vegetation indices and crop phenology metrics. *Agric. For. Meteorol.* **2013**, *173*, 74–84, doi:10.1016/j.agrformet.2013.01.007.
27. Ihuoma, S.O.; Madramootoo, C.A. Crop reflectance indices for mapping water stress in greenhouse grown bell pepper. *Agric. Water Manag.* **2019**, *219*, 49–58, doi:10.1016/j.agwat.2019.04.001.
28. Gong, Y.; Duan, B.; Fang, S.; Zhu, R.; Wu, X.; Ma, Y.; Peng, Y. Remote estimation of rapeseed yield with unmanned aerial vehicle (UAV) imaging and spectral mixture analysis. *Plant Methods* **2018**, *14*, 1–14, doi:10.1186/s13007-018-0338-z.
29. Ahmed, I.; ur Rahman, M.H.; Ahmed, S.; Hussain, J.; Ullah, A.; Judge, J. Assessing the impact of climate variability on maize using simulation modeling under semi-arid environment of Punjab, Pakistan. *Environ. Sci. Pollut. Res.* **2018**, *25*, 28413–28430, doi:10.1007/s11356-018-2884-3.
30. da Silva, E.E.; Rojo Baio, F.H.; Ribeiro Teodoro, L.P.; da Silva Junior, C.A.; Borges, R.S.; Teodoro, P.E. UAV-Multispectral and vegetation indices in soybean grain yield prediction based on in situ observation. *Remote Sens. Appl. Soc. Environ.* **2020**, *18*, *100318*, doi:10.1016/j.rsase.2020.100318.
31. Guo, Y.; Chen, S.; Li, X.; Cunha, M.; Jayavelu, S.; Cammarano, D.; Fu, Y. Machine Learning-Based Approaches for Predicting SPAD Values of Maize Using Multi-Spectral Images. *Remote Sens.* **2022**, *15*, 1337, doi:10.3390/rs12030514.
32. López-Calderón, M.J.; Estrada-ávalos, J.; Rodríguez-Moreno, V.M.; Mauricio-Ruvalcaba, J.E.; Martínez-Sifuentes, A.R.; Delgado-Ramírez, G.; Miguel-Valle, E. Estimation of total nitrogen content in forage maize (*Zea Mays* l.) Using Spectral Indices: Analysis by Random Forest. *Agric.* **2020**, *10*, 1–15, doi:10.3390/agriculture10100451.
33. Fawcett, D.; Panigada, C.; Tagliabue, G.; Boschetti, M.; Celesti, M.; Evdokimov, A.; Biriukova, K.; Colombo, R.; Miglietta, F.; Rascher, U.; et al. Multi-scale evaluation of drone-based multispectral surface reflectance and vegetation indices in operational conditions. *Remote Sens.* **2020**, *12*, doi:10.3390/rs12030514.
34. Achicanoy, J.A.; Rojas-Robles, R.; Sánchez, J.E. Análisis y proyección de las coberturas vegetales mediante el uso de sensores remotos y sistemas de información geográfica en la localidad de Suba, Bogotá-Colombia. *Gestión y Ambient.* **2018**, *21*, 41–58, doi:10.15446/ga.v21n1.68285.
35. Peñuelas, J.; Gamon, J.A.; Griffin, K.L.; Field, C.B. Assessing community type, plant biomass, pigment composition, and photosynthetic efficiency of aquatic vegetation from spectral reflectance. *Remote Sens. Environ.* **1993**, *46*, 110–118, doi:10.1016/0034-4257(93)90088-F.
36. Gitelson, A.A.; Kaufman, Y.J.; Merzlyak, M.N. Use of a green channel in remote sensing of global vegetation from EOS- MODIS. *Remote Sens. Environ.* **1996**, *58*, 289–298, doi:10.1016/S0034-4257(96)00072-7.
37. Gitelson, A.A.; Gritz, Y.; Merzlyak, M.N. Relationships between leaf chlorophyll content and spectral reflectance and algorithms for non-destructive chlorophyll assessment in higher plant leaves. *J. Plant Physiol.* **2003**, *160*, 271–282, doi:10.1078/0176-1617-00887.

38. Pearson, R.L.; Miller, L.D. Remote mapping of standing crop biomass for estimation of the productivity of the shortgrass Prairie. *Remote Sens. Environ. VIII* **1972**, *1*, 1355. Available online: https://ui.adsabs.harvard.edu/abs/1972rse..conf.1355P/abstract (accessed on 10 April 2022).
39. Gitelson, A.; Merzlyak, M.N. Quantitative estimation of chlorophyll-a using reflectance spectra: experiments with autumn chestnut and maple leaves. *J. Photochem. Photobiol. B Biol.* **1994**, *22*, 247–252, doi:10.1016/1011-1344(93)06963-4.
40. Vincini, M.; Frazzi, E.; D'Alessio, P. A broad-band leaf chlorophyll vegetation index at the canopy scale. *Precis. Agric.* **2008**, *9*, 303–319, doi:10.1007/s11119-008-9075-z.
41. Guan, L.; Liu, X.N.; Cheng, C.Q. Research on hyperspectral information parameters of chlorophyll content of rice leaf in cd-polluted soil environment. *Guang Pu Xue Yu Guang Pu Fen Xi/Spectroscopy Spectr. Anal.* **2009**, *29*, 2713–2716, doi:10.3964/j.issn.1000-0593(2009)10-2713-04.
42. Alam, M.J.; Rahman, K.M.; Asna, S.M.; Muazzam, N.; Ahmed, I.; Chowdhury, M.Z. A Soil-Adjusted Vegetation Index (SAVI). *Remote Sens. Environ.* **1988**, *25*, 295–309, doi:10.1016/0034-4257(88)90106-X.
43. Raper, T.B.; Varco, J.J. Canopy-scale wavelength and vegetative index sensitivities to cotton growth parameters and nitrogen status. *Precis. Agric.* **2015**, *16*, 62–76, doi:10.1007/s11119-014-9383-4.
44. R Core Team. *R: A Language and Environment for Statistical Computing*. R Foundation for Statistical Computing: Vienna, Austria, **2021**. Available online: https://www.r-project.org/ (accessed on 12 November 2021).
45. Le, S.; Josse, J.; Huaaon, F. FactoMineR: An R package for multivariate analysis. *JournalofStatisticalSoftware.* **2008**, *25*, 1–18, doi:10.18637/jss.v025.i01.
46. Wickham, H. *Ggplot2: Elegant Graphics for Data Analysis*; Springer-Verlag, Ed.; Secund edi.; New York, 2016.
47. Kassambara, A.; Mundt, F. *Package "Factoextra"*. Available online: https://cran.r-project.org/web/packages/factoextra/factoextra.pdf (accessed on 12 November 2021).
48. Schloerke, B.; Cook, D.; Larmarange, J.; Briatte, F.; Marbach, M.; Thoen, E.; Elberg, A.; Crowley, J. *Package "GGally"*. Available online: https://cran.r-project.org/web/packages/GGally/GGally.pdf (accessed on 12 November 2021).
49. Miscellaneous, T.H.; Yes, L. Package "Hmisc". Available online: https://cran.r-project.org/web/packages/Hmisc/Hmisc.pdf (accessed on 12 November 2021).
50. Package, T.; Mendiburu, A.F. Package "agricolae". Available online: https://cran.r-project.org/web/packages/agricolae/agricolae.pdf (accessed on 12 November 2021).
51. Pudelko, R.; Stuczynski, T.; Borzecka-Walker, M. The Suitability of an Unmanned Aerial Vehicle (UAV) for the Evaluation of Experimental Fields and Crops. *Zemdirbyste* **2012**, *99*, 431–436.
52. MIDAGRI. Perfil productivo y competitivo de los principales cultivos del sector. Available online: https://acortar.link/fjrSc (accessed on 11 April 2021).
53. Gavilánez-Luna, F.C.; Gómez-Vargas, M.J. Definición de dosis de nitrógeno, fósforo y potasio para una máxima producción del maíz híbrido Advanta 9313 mediante el diseño central compuesto. *Cienc. Tecnol. Agropecu.* **2022**, *23*, doi:10.21930/rcta.vol23_num1_art:2225.
54. Farmagro. Maíz Adv 9313. Available online: http://www.farmagro.com.pe/p/advanta-9313/ (accessed on 6 April 2022).
55. Jin, X. liang; Diao, W. ying; Xiao, C. hua; Wang, F. yong; Chen, B.; Wang, K. ru; Li, S. Shao-kun. Estimation of Wheat Agronomic Parameters Using New Spectral Indices. *PLoS One.* **2013**, *8*, doi:10.1371/journal.pone.0072736.
56. Gómez-Candón, D.; Virlet, N.; Labbé, S.; Jolivot, A.; Regnard, J.L. Field phenotyping of water stress at tree scale by UAV-sensed imagery: new insights for thermal acquisition and calibration. *Precis. Agric.* **2016**, *17*, 786–800, doi:10.1007/s11119-016-9449-6.
57. Barzin, R.; Pathak, R.; Lotfi, H.; Varco, J.; Bora, G.C. Use of UAS multispectral imagery at different physiological stages for yield prediction and input resource optimization in corn. *Remote Sens.* **2020**, *12*, doi:10.3390/RS12152392.
58. Suno, S.; Cho, J.; Guinness, J.; van Aardt, J.; Czymmek, K.J.; Ketterings, Q.M. Corn grain yield prediction and mapping from Unmanned Aerial System (UAS) multispectral imagery. *Remote Sens.* **2021**, *13*, doi:10.3390/rs13193948.
59. Ahmad, I.; Singh, A.; Fahad, M.; Waqas, M.M. Remote sensing-based framework to predict and assess the interannual variability of maize yields in Pakistan using Landsat imagery. *Comput. Electron. Agric.* **2020**, *178*, 105732, doi:10.1016/j.compag.2020.105732.
60. Hassan, M.A.; Yang, M.; Rasheed, A.; Yang, G.; Reynolds, M.; Xia, X.; Xiao, Y.; He, Z. A rapid monitoring of NDVI across the wheat growth cycle for grain yield prediction using a multi-spectral UAV platform. *Plant Sci.* **2019**, *282*, 95–103, doi:10.1016/j.plantsci.2018.10.022.
61. Peroni, L.; Chartuni, E.; do Amaral, C.H.; Usher, C.M.; Zution, I.; Filgueiras, R.; Coelho, F. Potential of using spectral vegetation indices for corn green biomass estimation based on their relationship with the photosynthetic vegetation sub-pixel fraction. *Agric. Water Manag.* **2020**, *236*, 106155, doi:10.1016/j.agwat.2020.106155.
62. Zenteno, G.A.; Palacios, E.; Tijerina, L.; Flores, H. Aplicación de tecnologías de percepción remota para la estimación del rendimiento en caña de azúcar. *Revista mexicana de ciencias agrícolas*. **2017**, 8, 1575-1586.
63. Montealegre, F.A. Evaluación espacio temporal de la productividad agrícola con índices de vegetación de diferencias normalizadas (NDVI) Como herramienta para el ordenamiento territorial. Caso de estudio cuenca Alta del Arroyo Napaleofú, Provincia de Buenos Aires, Argentin, Universidad Nacional de la Plata, **2017**.

 doi:10.20944/preprints202205.0231.v1

64. Zhou, X.; Kono, Y.; Win, A.; Matsui, T.; Tanaka, T.S.T. Predicting within-field variability in grain yield and protein content of winter wheat using UAV-Based multispectral imagery and machine learning approaches. *Plant Prod. Sci.* **2021**, *24*, 137–151, doi:10.1080/1343943X.2020.1819165.